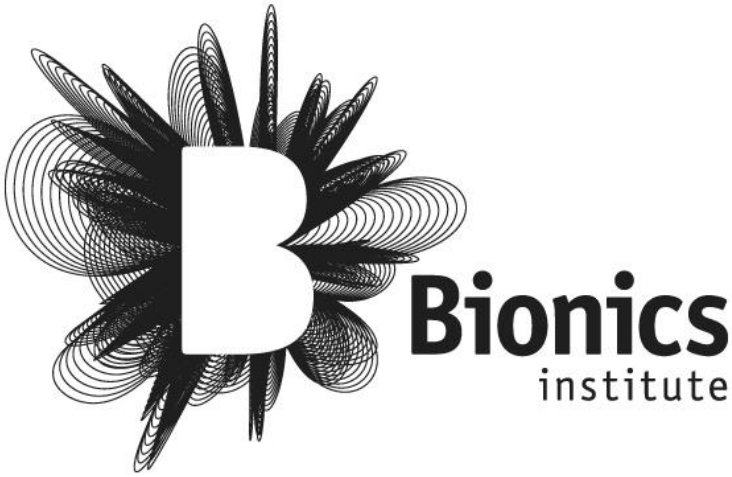

Visual cortex responses to suprachoroidal electrical stimulation of the retina: effects of electrode return configuration

Running Head: Visual cortex response to suprachoroidal stimulation

Rosemary Cicione[1,2], Mohit N Shivdasani[1], James B Fallon[1], Chi D Luu[3], Penny J. Allen[3], Graeme D Rathbone[1,2], Robert K Shepherd[1] and Chris E Williams[1]

[1]Bionics Institute, VIC-3002, Australia

[2]Department of Electronic Engineering, La Trobe University, VIC-3086, Australia

[3]Centre for Eye Research Australia, University of Melbourne, Royal Victorian Eye & Ear Hospital, VIC 3002, Australia

Corresponding Author:

A Prof. Chris E Williams

Bionics Institute, 384-388 Albert Street, East Melbourne, VIC – 3002, AUSTRALIA

Tel: +61-3-92883523

Fax: +61-3-92882998

Email: cwilliams@bionicsinstitute.org

Abstract

A clinically effective retinal prosthesis must evoke localized phosphenes in a retinotopic manner in response to stimulation of each of the retinal electrodes, evoke brightness cues over a wide dynamic range and function within safe stimulus limits. The effects of varying return configuration for retinal stimulation are currently unknown. To investigate this, we implanted a flexible, 7x12 electrode array into the suprachoroidal space of normally-sighted, anesthetized cats. Multi-unit activity in the primary visual cortex was recorded in response to electrical stimulation using various return configurations: monopolar vitreous (MPV), common ground (CG), hexagonal (HX), monopolar remote (MPR) and bipolar (BP_*N*). MPV stimulation was found to be the most charge efficient and was most likely to induce cortical activity within safe charge limits. HX and CG stimulation were found to exhibit greater retinal selectivity compared to the MPV return at the expense of lower cortical yield and higher P50 charge levels, while cortical selectivity was unaffected by choice of return. Responses using MPR and widely spaced BP_*N* configurations were similar to those using the MPV return. These results suggest that choice of return configuration for a retinal prosthesis will be balanced between resolution and stimulation within safe charge limits.

Introduction

Retinitis Pigmentosa (RP) is a genetic disorder affecting approximately 1 in 4000 people worldwide (Hartong et al. 2006). The disease is characterized by the progressive loss of photoreceptors in the retina and results in severe vision impairment (Hartong et al. 2006). Currently, there is no effective treatment for RP, providing the impetus for research into retinal prostheses.

Four sites of placement of a retinal electrode array have been investigated: epiretinal attachment directly onto the surface of the inner retina (Eckmiller 1997, Mokwa et al. 2008, Humayun et al. 2009), subretinal placement between the choroid and photoreceptors (Zrenner et al. 1997, Kelly et al. 2009, Gekeler et al. 2010), suprachoroidal implantation between the sclera and choroid (Kanda et al. 2004, Zhou et al. 2008, Wong et al. 2009, Shivdasani et al. 2010) and the trans-scleral approach whereby the stimulating electrodes penetrate the retina through the sclera, choroid and retinal pigment epithelium (Gerding 2007). Regardless of the approach taken, the goal is to electrically stimulate surviving retinal ganglion cells in order to create percepts that convey information about the visual scene.

Initial investigations into the ability of retinal stimulation to produce percepts in humans have reported that subjects see bright spots of light, termed phosphenes, whose size as well as level of brightness increases with increasing stimulating charge (Humayun et al. 1999, Humayun et al. 2003, Rizzo et al. 2003, 2003, De Balthasar et al. 2008, Fujikado et al. 2011, Wilke et al. 2011). It is anticipated that activation of multiple electrodes on a two-dimensional retinal electrode array will provide a phosphenized reconstruction of simple objects (Humayun et al. 1999). In order to achieve this goal, it is important to consider the following: a) the stimulus levels required to induce a phosphene need to be maintained below levels that induce damage for both retinal tissue and the stimulating electrodes, b) a large dynamic range of electrical stimulation and large number of distinguishable brightness levels are desirable in order to sufficiently modulate the perceived intensity of the phosphenes comprising the image and c) stimulation of electrodes on the array should produce localized phosphenes in a retinotopic manner to facilitate a distinct representation of the visual scene.

Cochlear implant (CI) studies show that the electrode return configuration used during electrical stimulation influences both the threshold and spatial distribution of induced multi-unit activity (MUA) in the auditory cortex of animals (Bierer and Middlebrooks 2002, Snyder et al. 2008, Fallon et al. 2009), as well as perceptual thresholds in humans (Busby et al. 1994, Pfingst et al. 1995, Pfingst et al. 1997, Bierer 2007). These studies have demonstrated that greater spatial selectivity can be achieved at the expense of higher threshold by varying the electrode return configuration. For example, narrow return configurations such as bipolar and tripolar returns create more focused current fields in the cochlea compared to wide return configurations like the monopolar return (Van Den Honert and Stypulkowski 1987, Jolly et al. 1996, Kral et al. 1998). This in turn may result in the excitation of a more confined area of neurons in the auditory cortex, resulting in an expected improvement in speech recognition over that using the monopolar return (Bierer and Middlebrooks 2002, Snyder et al. 2008). However, whilst it has been demonstrated that narrow electrode return configurations can provide more localized information to higher auditory structures, enhanced speech recognition is not necessarily achieved in CI recipients using such configurations (Zwolan et al. 1996, Pfingst et al. 1997).

To date, human clinical trials with retinal prostheses have been conducted by a number of groups utilizing either epiretinal (Yanai et al. 2007, De Balthasar et al. 2008, Klauke et al. 2011), subretinal (Rizzo et al. 2003a, b, Wilke et al. 2011, Zrenner et al. 2010) or suprachoroidal (Fujikado et al. 2011) placements. These trials have confirmed that phosphenes can be induced within safe charge limits for stimulation of the retina using either monopolar or bipolar return configurations. However, it is believed that a suprachoroidal electrode placement is likely to result in higher thresholds and lower resolution compared to both epiretinal and subretinal prostheses due to the increased distance between the electrode array and the retina (Kanda et al. 2004, Fujikado et al. 2011). Therefore, the choice of electrode return configuration is expected to be an important factor in determining the resolution achievable with suprachoroidal stimulation (Wong et al. 2009).

In the present study, we characterized the effect of electrode return configuration on MUA in the visual cortex using suprachoroidal electrical stimulation of the retina. In particular, we compared the

efficacy of the monopolar return with narrower configurations such as the bipolar and common ground return. For bipolar stimulation, either the electrode immediately adjacent to the stimulating electrode or an electrode separated by some distance from the stimulating electrode is chosen as the return. With a common ground return, the active electrode is stimulated against all remaining electrodes on the array shorted together. While there may be complexities associated with using the common ground return configuration as a result of variations in the spatial arrangement of the return electrodes, particularly with electrodes on the edges of the array, we chose to include this configuration for the following reasons. Firstly, both bipolar and common ground returns have been shown to provide spatial selectivity in CI patients (Busby et al. 1994) and are used clinically where monopolar stimulation may not be viable. Secondly, with bipolar stimulation, it is possible to evoke neural activity from both the cathodic and anodic phases of stimulation whereas the common ground return may result in a more restricted excitation, as the return current is spread across a larger surface area. Finally, the common ground return is also a valuable tool for fault detection in a stimulating electrode array and is able to identify shorts between electrodes (John et al. 2011). Another electrode return configuration of interest was the hexagonal return, particularly relevant to retinal prostheses (Suaning and Lovell 2006). For the hexagonal return configuration, a ring of six guard electrodes surrounding the stimulating electrode serve to capture injected charge, thereby potentially restricting activation to a confined area (Dommel et al. 2005, Dommel and Et Al. 2009, Wong et al. 2009). For each of these electrode return configurations, we compared the charge levels required to elicit cortical activation, dynamic ranges, retinal selectivity and cortical selectivity.

Materials and Methods

Anaesthesia and Surgery

Experiments were performed on normally-sighted adult cats (n=7) with approval from the Royal Victorian Eye and Ear Hospital Animal Ethics Committee. Prior to surgery, animals were injected with ketamine (intramuscular, i.m., 20 mg kg^{-1}) and xylazil (subcutaneous, s.c., 2 mg kg^{-1}). A continuous intravenous injection of sodium pentobarbitone (60 mg kg^{-1}) was used to maintain anesthesia over the duration of the experimental period of 3-4 days. Vital signs (respiration rate, end tidal CO_2 and temperature) were monitored throughout the experiment. An infusion of sodium lactate (Hartmann's solution, 2 ml kg^{-1} hr^{-1}) was administered throughout the experiment as well as daily injections of Dexamethasone (i.m. 0.1 mg kg^{-1}) and Clavulox (s.c. 10 mg kg^{-1}).

Details of the suprachoroidal surgical implantation have been described previously (Shivdasani et al. 2010). All surgeries were conducted by an experienced retinal surgeon. Briefly, a lateral canthotomy was performed to obtain temporal access to the eye. An incision was then made through the sclera adjacent to the limbus and a surgical blade used to create a pocket between the sclera and choroid. The electrode array, (figure 1(a)) was inserted approximately 15-17mm into the suprachoroidal space (figure 1(b) and 1(c)) with the tip of the array positioned beneath the area centralis (5/7 cats), (Villalobos et al. 2011). The array was then sutured to the sclera for stability. Placement of the retinal implant relative to the optic disk was confirmed with a fundus image (figure 1(b)). The fundus image was captured through the view of a quadraspheric fundus lens (Volk Optical, Mentor, OH) with a camera (AxioCam ICC3, Carl Zeiss Technologies) attached to the surgical microscope. Only one eye was implanted for each animal.

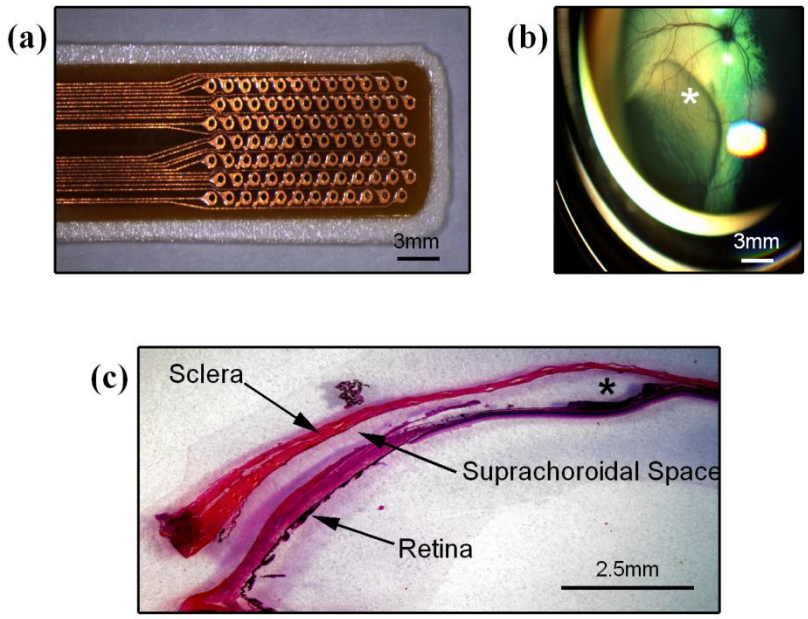

Figure 1: *Experimental setup. (a) A silicon coated polyimide array with platinum electrodes (electrode diameter: 400µm) arranged in 7 rows by 12 columns. (b) Fundus image verifying placement of the array in the suprachoroidal space. (c) A histological slice through the retina displaying the electrode pocket formed in the suprachoroidal space as a result of the electrode array insertion. The location of the tip of the array is indicated by the asterisk in (b) and (c).*

After surgery, the animal was placed in a stereotaxic frame using solid ear bars (David Kopf Instruments, Tujunga, CA) and a craniotomy spanning 15mm rostral and 5mm caudal from the inter-aural line, and 6mm on either side of the midline was performed to expose the primary visual cortex (V1) (Snider and Niemer 1961). Using a platinum ball electrode, electrically evoked potentials were mapped every 0.5-1mm on the dorsal surface of V1 along the medial gyrus in the rostro-caudal direction, while simultaneously stimulating a column of retinal electrodes using cathodic-first, biphasic pulses, 500µs per phase, 0-2mA (Shivdasani et al. 2010). This procedure was performed in both cortices. The cortical area with the lowest evoked potential threshold to electrical stimulation was chosen to implant a multichannel recording electrode. Typically, implantation occurred in the hemisphere contralateral to the eye used for electrical stimulation in the area that corresponded

reasonably well with the location of the tip of the retinal array in the visual space, based on the fundus image (Tusa et al. 1978).

Suprachoroidal Electrode Array

The retinal array (figure 1(a)) consisted of a flexible, polyimide substrate with 7 rows x 12 columns of 400µm-diameter electroplated platinum electrodes, designed in-house for acute experiments and manufactured by Flexible Circuit Technologies (Plymouth, MN). The electrodes had a center-to-center separation of 1.0 mm along each row and 0.8 mm along each column, equivalent to approximately 4° visual angle in the cat (Hubel and Wiesel 1959). The underside and edges of the array were coated in biocompatible silicon (Permatex, CT; Type 65AR flowable). A Dacron patch was glued approximately 17mm from the tip to enable suturing of the array to the sclera.

Multichannel Recording Electrodes

Neural activity was recorded with either a 32-channel (4-shank x 8-electrode) silicon substrate array (NeuroNexus Technologies, Ann Arbor, MI) or a planar 49 (7x7) or 60 (6x10)-channel array (Blackrock Microsystems, Foxborough, MA). The shanks on the silicon substrate array were separated by a distance of 400µm, and the distance between each electrode on a shank was 200µm. These arrays sampled approximately 1.2mm of cortical space in the rostro-caudal direction and were inserted to an average depth of 2500µm below the dorsal surface of V1. The electrodes on the planar array were separated by a distance of 400µm and thus sampled a larger area (2.5mm medio-lateral direction, 4mm rostro-caudal direction) of cortical space compared to the silicon substrate arrays. These arrays penetrated the cortex to a depth of approximately 1mm.

Electrical Stimulation and Recording Protocols

Experiments were conducted in a darkened, electrically shielded Faraday room. . The Cerebus recording system (Blackrock Microsystems, Salt Lake City, Utah) was used to record continuous MUA across all channels at a sampling frequency of 30 kHz. All electrical stimuli were generated with an in-house built, optically isolated constant current stimulator. Electrodes were stimulated with cathodic-first, charge balanced biphasic pulses. The duration of each phase and the interphase gap were kept constant at 500μs per phase and 25μs respectively. Pulses were presented at a rate of 1Hz. Current varied randomly from zero to 725μA in 25μA steps with each current level repeated 10 times. The maximum stimulating current of 725μA ensured that charge densities were below 300μC cm^{-2}, the limit deemed safe for platinum electrodes based on electrochemical considerations (Brummer and Turner 1977).

A custom, automated switching system (John et al. 2011) was used to stimulate individual electrodes on the suprachoroidal array with various return configurations. The electrode return configurations tested were: a) monopolar vitreous (MPV), whereby the return was a platinum ball electrode placed in the vitreous humor (figure 2(a)), b) monopolar remote (MPR) whereby the return was an electrode inserted either in the conjunctiva or placed in a skinfold in the shoulder (figure 2(a)), c) bipolar (BP_*N*) where an electrode on the same row as the active electrode was used as a return (figure 2(b)) d) common ground (CG) where 19 electrodes along the columns closest to the active electrode on the array were shorted together to form the return (figure 2(c)) and e) hexagonal (HX) where the return consisted of six electrodes surrounding the active electrode on the array (figure 2(d)).

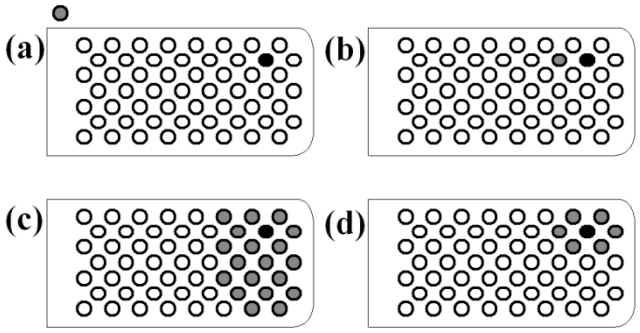

Figure 2: *Electrode return configurations. The stimulating electrode is shown in black and the return electrode(s) in gray. (a) Monopolar return electrode placed either in the vitreous humor (MPV) or extraocularly (MPR). (b) BP_N stimulation, shown for the case BP_1. The return electrode was incrementally shifted further away from the stimulating electrode. (c) The Common Ground (CG) configuration where the return was formed by the 19 electrodes closest to the stimulating electrode. (d) Hexagonal (HX) configuration whereby the stimulating electrode is surrounded by six return electrodes.*

The main focus of the study was to compare cortical responses to stimulation using the MPV return against the CG and HX configurations. Only those electrodes which were able to form a complete HX were stimulated. However, as the MPV return required an additional electrode to be placed inside the eye, it was important to assess the effect of the location of the monopolar return on cortical responses. Therefore in some animals, we compared responses to stimulation using the MPV return against those using the MPR return. Furthermore, to assess whether a return electrode could be placed on the suprachoroidal array itself, responses using the MPV return were compared to those using the BP_*N* configuration. For the BP_*N* configuration, multiple recordings were made while incrementally varying the distance between the active and return electrodes on the array. This equates to a center-to-center separation, *N*, of 1mm up to 11mm (an example of BP_1 is shown in figure 2(b)). Only BP_*N* configurations with a center-to-center separation of up to 8mm were included in the analysis.

Data Analysis

Offline processing using custom scripts created in Igor Pro (Wavemetrics, Lake Oswego, OE) was used to identify spikes on each cortical channel. Signal artifacts from electrical stimulation were first removed using the methods described in Heffer and Fallon (2008). The signal was then band-pass filtered (Butterworth filter, frequency: 0.3-5kHz, order: 3) and a root mean square (RMS) estimate was made every 60 seconds using a moving time window. Spikes were detected if the signal exceeded

four times the RMS value within a given 60-second window (figure 3(a)). Figure 3(b) shows a peri-stimulus time histogram (PSTH) from a single cortical channel in response to electrical stimulation of a retinal electrode using the MPV configuration. Typically, MUA in V1 occurred approximately 3-20ms post stimulation. However, in some instances, this initial burst was followed by a secondary burst of spiking activity at latencies greater than 30ms (figure 3(b)). The presence of this two phased response with early and late components was not influenced by the electrode return configuration. Therefore, we chose to analyze only the early component, consistent with what has been done in previous retinal stimulation studies (Wong et al. 2009, Shivdasani et al. 2010).

P50 Charge Level, Dynamic Range and Discrimination Index

For each retinal electrode stimulated, a spike rate versus current plot (examples in figure 3(c)) was derived for all recording sites in V1 by analyzing spikes occurring within 3-20ms post-stimulus onset. Sigmoid curves were fitted to the spike rate plots and only those plots in which a saturating rate response was observed were included in further analyses. From the fitted sigmoid, the current at which spike rate was found to be half of the maximum saturating spike rate, expressed as charge per phase in nC (P50, figure 3(c)) was calculated. This P50 charge level was used to compare the charge required to evoke cortical MUA across return configurations. The reason for comparing charge at the 50% activation point is because it is the steepest point on the sigmoid curve and therefore has the least error in estimation. Previous studies employing CI stimulation have defined this level as threshold (Fallon et al. 2009). For each retinal electrode stimulated, the best cortical electrode (BCE), defined as the recording site in V1 with the lowest P50 charge level was found. Dynamic range (presented in dB) was calculated as the log ratio of the currents eliciting 90% (P90) and 10% (P10) of the maximum saturating spike rate (figure 3(c)), (Fallon et al. 2009). In this manner, the dynamic range describes the likely operational stimulating range for each retinal electrode. However, it gives no indication as to whether or not two different current levels can produce distinguishable spiking responses, and potentially, two perceptually distinguishable brightness levels. Therefore the discrimination index, d`,

derived from a receiver operator characteristic (ROC, Macmillan and Creelman (2005)) curve was used to determine whether spike rates from adjacent current steps were distinguishable. The ROC curve was generated based on spiking activity from current levels 25μA (the minimum current step) above and below the P50 current level of the BCE. These stimulus levels were chosen as the input-output function is steepest in this region and therefore stimuli should be most distinguishable. To calculate d`, the area under the ROC curve was converted to its equivalent standard deviate and the resulting z-score was multiplied by √2 (Middlebrooks and Snyder 2007). If the area under the ROC curve was calculated to be one, a proportion of 1-1/(2N), where N is the number of points on the ROC curve, was used to compute the z-score (Macmillan and Creelman 2005).For each retinal electrode stimulated, the P50 charge level, dynamic range and d' of the BCE were analyzed and compared across electrode return configurations.

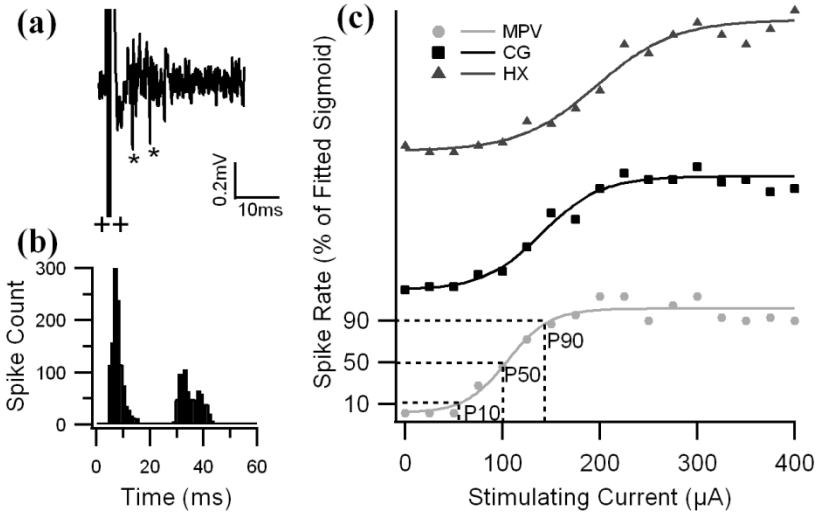

Figure 3: *Example of electrically evoked MUA in the visual cortex. (a)Typical recording of cortical multi-unit activity in response to stimulation of a single retinal electrode demonstrating stimulus artifact (++) and spiking activity post-stimulus (*). (b) Post-stimulus time histogram of spiking activity for stimulation of a single retinal electrode across all current levels. (c) Normalized spike rate versus stimulating current level function with the symbols indicating raw spike count for each current level in the window 3-20ms post-stimulus onset (shown only for current levels up to 400μA). Fitted sigmoid functions for each of MPV (circle), CG (square) and HX (triangle) return configurations are*

also shown. P10, P50 and P90 current levels are indicated on the MPV sigmoid curve only. Data for the CG and HX curves have been displaced along the ordinate for clarity.

Retinal Selectivity

For each cortical recording site, the best retinal electrode (BRE; defined as the stimulating electrode in the retina which yielded the lowest P50 charge level) was identified. In order to assess the retinal spread of activation for each cortical recording site, we analyzed spike rates evoked by stimulation of electrodes across the retinal array at a near saturating charge level (P90 of the BRE). All spike rates were normalized to that evoked by stimulation of the BRE. In order to quantify the degree of retinal selectivity, the reduction in spike rate that resulted from moving the stimulating electrode one electrode site away from the BRE were compared.

Cortical Selectivity

As a measure of cortical spread of activation for each retinal electrode, spike rates across the cortical recording array at a near saturating charge level (P90 of the BCE) were analyzed as a function of distance in the cortex from the BCE. Absolute spike rates at the defined charge level were normalized to the maximum spiking level for that cortical site after subtracting the spontaneous spike rate as per Bierer and Middlebrooks (2002). A decaying exponential function was fitted to the data points and the inverse decay constant, $1/\tau$, of the fitted exponential function was used to quantify cortical selectivity. Only those retinal electrodes in which MUA was recorded with the planar array were included for cortical selectivity analysis.

Statistical Analyses

All statistical analyses were performed using SigmaPlot (Systat Software, San Jose, CA). Comparisons of P50 charge level, dynamic range, d` and the selectivity measures for MPV vs. CG vs. HX returns and for MPV vs. BP_*N* returns were performed using one-way repeated measures ANOVAs. Where appropriate, post-hoc differences amongst the individual returns were computed using the Tukey test. Post-hoc differences between individual BP_*N* returns to the MPV return were performed with the Holm-Sidak method. Paired t-tests were used to compare MPV vs. MPR data. All values are reported as mean ± standard deviation.

Results

Time constraints made it impossible to electrically stimulate all 84 electrodes on each of the implanted suprachoroidal arrays. Across all seven animals, 103 retinal electrodes were stimulated using the three major (MPV, CG and HX) electrode return configurations. From a cortical viewpoint, the overall yield of recording sites in which a P50 charge level was obtainable was 990 (22.0%, MPV), 535 (11.9%, CG) and 233 (5.2%, HX) out of a total of 4503 recording sites in V1. From a retinal viewpoint, the MPV return was observed to be the most efficacious in evoking recordable responses in V1 with identifiable BCEs for 68 electrodes compared to 53 and 31 electrodes for the CG and HX returns respectively. Only those electrodes in which a BCE was determined for all of the return configurations were included for P50 charge level, dynamic range, discriminability index and selectivity analyses (n=28). We found that the BCE was not necessarily unique to a given retinal electrode and showed some dependence on the electrode return configuration. For each of the MPV, CG and HX returns, 16, 14 and 8 retinal electrodes respectively were found to share the same BCE with at least one other retinal electrode. Similar inclusion criteria were adopted for the MPV vs. MPR analyses with 26 retinal electrodes analysed, while for the BP_*N* vs. MPV analyses, data from 12 retinal electrodes were included.

P50 Charge Level

As expected, the P50 charge level of the BCE showed a strong dependence on electrode return configuration (figure 4(a)), increasing from MPV to CG to HX. P50 for MPV stimulation was found to be lower than both CG and HX return configurations *($p < 0.001$)*. The CG return was found to elicit lower P50 values than the HX return *($p < 0.001$)*. Nevertheless, for all three electrode return configurations, charge densities required per phase to elicit both 50% and 90% cortical activation (table 1) were found to be well below the safe stimulation limit for platinum electrodes (Brummer and Turner 1977).

Table 1: *Charge densities required (mean ± SD μC cm^{-2}) for 50% (P50) and 90% (P90) cortical activation. Values at P90 are indicative of the stimulating intensity range required for each of the electrode return configurations.*

	BCE	
Return	**P50**	**P90**
MP	64±36	97±59
CG	105±49	155±66
HX	140±66	182±70

The P50 charge levels of the BCE obtained with the differing locations of the monopolar return electrode are illustrated in figure 4(b). MPV and MPR returns were not found to be significantly different from each other.

P50 charge levels of the BCE obtained with BP_*N* stimulation are presented in figure 4(c). There was a trend of decreasing P50 charge with increasing active-return electrode separation up to 4mm (BP_4) after which a plateau in the P50 value was observed. Comparison of individual BP_*N* configurations to the MPV return revealed that the mean P50 for BP_1 and BP_2 were higher than that with the MPV return ($p < 0.001$ and $p < 0.05$ respectively). For all remaining BP_*N* configurations, the P50 charge levels were not significantly different to those obtained with MPV stimulation.

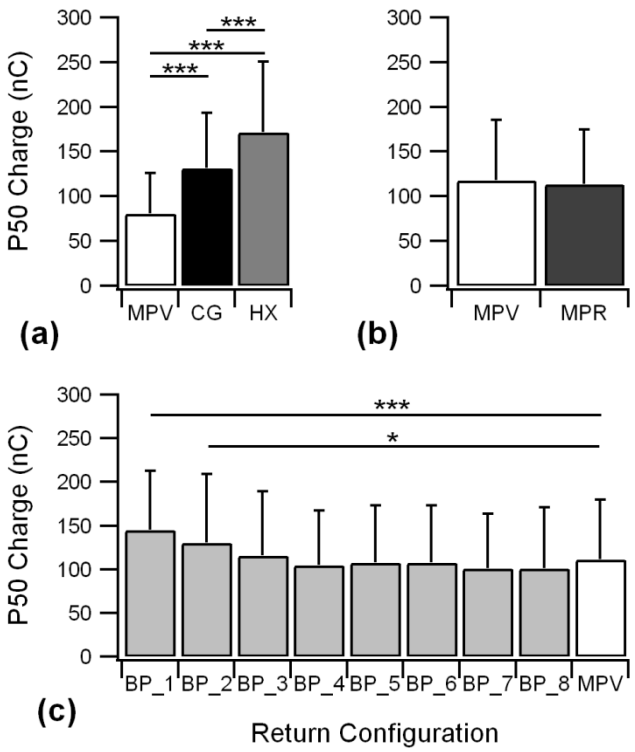

Figure 4: *P50 charge per phase levels (mean + SD) of the BCE. (a) P50 charge levels for the MPV, CG and HX return configurations. (b) P50 charge levels for the alternate locations of the monopolar return. (c) P50 charge for BP_N and MPV return configurations. * $p < 0.05$; *** $p < 0.001$.*

Dynamic Range

The dynamic ranges of the BCE observed for MPV, CG and HX stimulation are presented in figure 5(a). There was no significant difference in the dynamic ranges between each of the three electrode return configurations. This was found as well for the MPV vs. MPR (figure 5(b)) and BP_*N* vs. the MPV return (figure 5(c)).

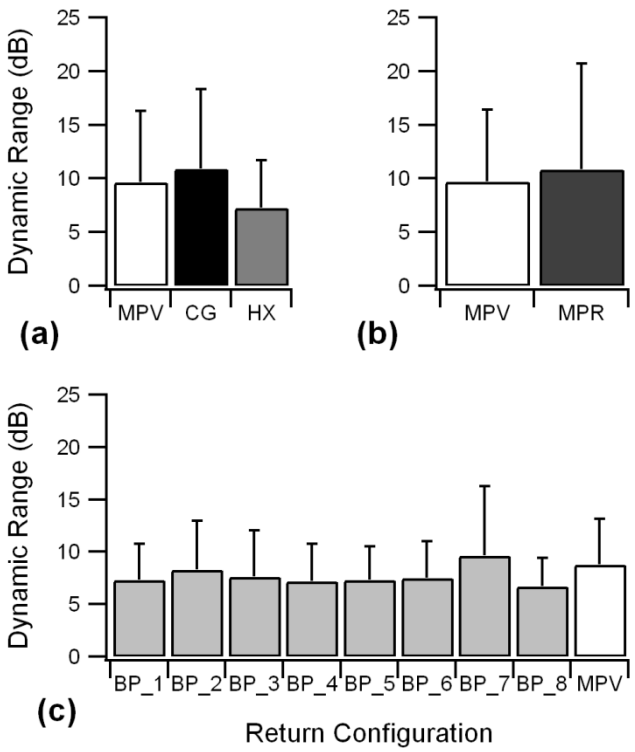

Figure 5: *Dynamic ranges (mean + SD) expressed as the log ratio between P90 and P10 current levels for (a) MPV versus CG versus HX, (b) MPV versus MPR and (c) BP_N versus MPV electrode return configurations. Dynamic range was not found to be affected by the electrode return configuration.*

Discriminability Index

A d` of zero indicates chance performance (Macmillan and Creelman 2005). For the data here, this would imply that there is no difference in the level of spiking activity produced when electrically stimulating at two different current levels, above and below P50, in this case separated by 50μA. As can be seen from figure 6, all electrode configurations showed a reasonable degree of discriminability. However, the MPV return was found to have a significantly higher d` compared to both the CG and HX returns (figure 6(a)) and the BP_1 return (figure 6(c)). Discrimination indices for the MPV and MPR return configurations (figure 6(b)) were not found to differ.

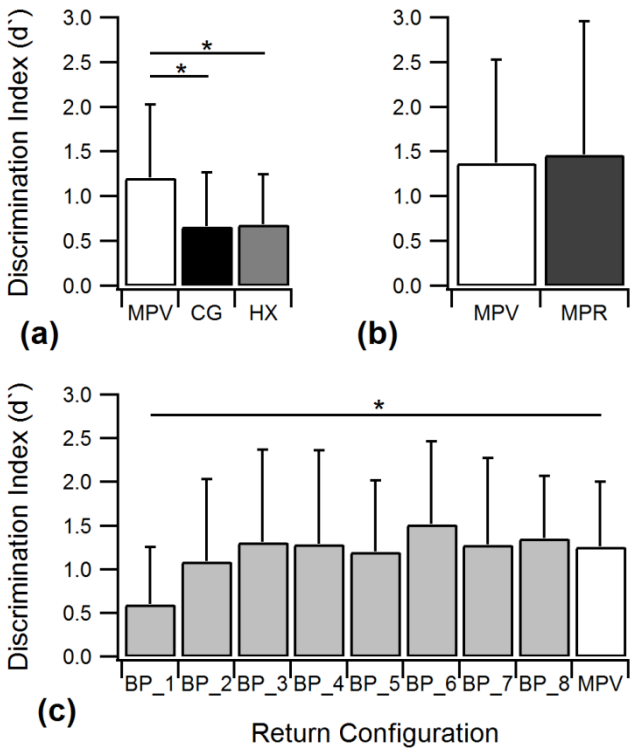

Figure 6: *Discrimination Indices (mean + SD) for (a) MPV versus CG versus HX, (b) MPV versus MPR and (c) BP_N versus MPV electrode return configurations. These were calculated near the P50 current for a 50μA current step. For the BP_N versus MPV comparison (c), 11/12 retinal electrodes were included for analysis as one retinal electrode was stimulated in current increments of 50μA. * p < 0.05.*

Retinal Selectivity

Retinal spread of activation and the resultant retinal selectivity was estimated and compared across the MPV, CG and HX return configurations only for those cortical sites in which a BRE could be identified. Typically, in each experiment only two retinal electrodes (out of 12-15 retinal electrodes which were generally stimulated) were identified to be the BRE for all cortical sites on the recording array. Occasionally in some experiments using the MPV and CG returns, 3 or 4 retinal electrodes were identified to be the BRE.

Figure 7 demonstrates how spiking activity recorded for a single cortical electrode varies in response to stimulation of several retinal electrodes at a near saturated level (P90) for the BRE. As the stimulating electrodes were moved further from the BRE, the level of MUA induced at the given cortical site decreased up to a distance of approximately 1.6 to 2 mm away from the BRE. Stimulation of retinal electrodes beyond this distance did not evoke any spiking activity for this cortical site.

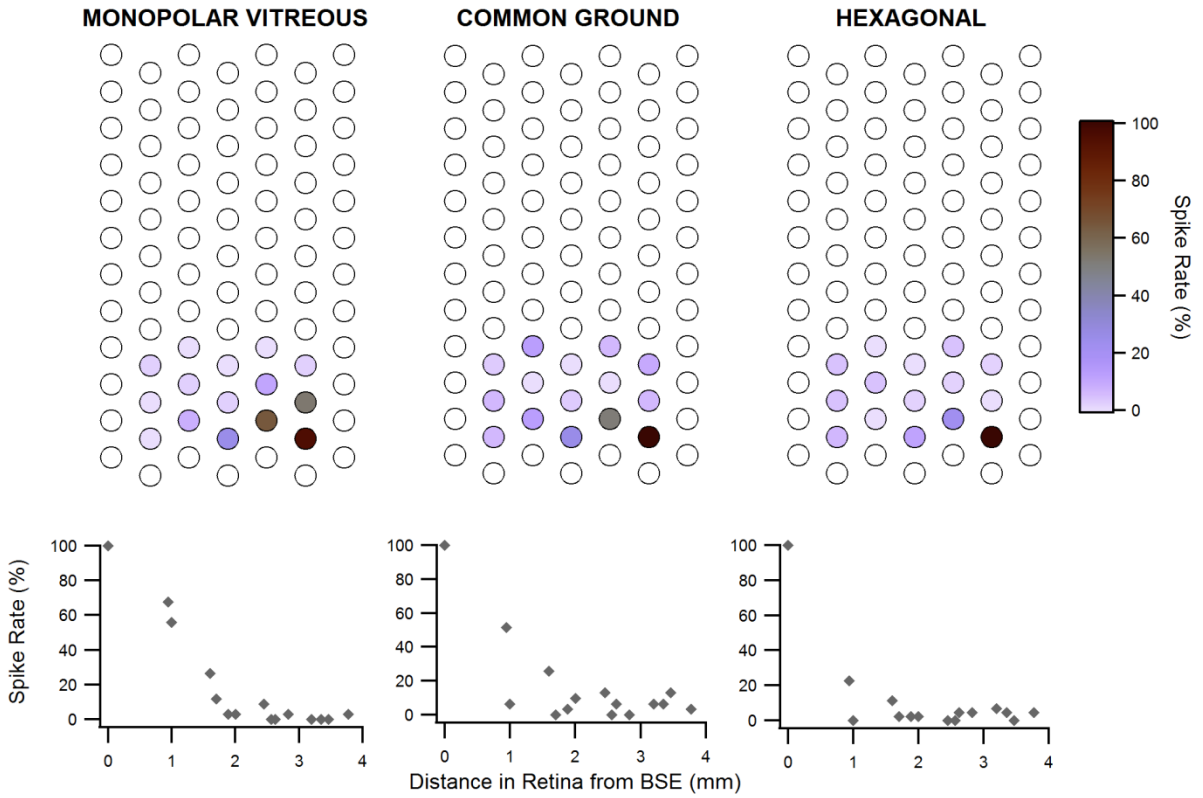

Figure 7: *Retinal spread of activation. The top panels show the percentage spike rate (%, color bar) normalized to the spike rate of the best stimulating electrode (BRE), observed for one cortical recording location using the MPV, CG and HX return configurations at the P90 current level of the BRE. The BRE is colored black. Open circles indicate electrodes which were not electrically stimulated. Beneath each image is a graph of spike rate as a function of the distance in the retina from the BRE (diamond symbols) used to estimate retinal selectivity.*

In order to assess retinal selectivity, we compared the drop in spike rate for retinal electrodes immediately adjacent to the BRE. A total of 191 cortical sites were included in the analysis of retinal

selectivity (figure 8(a)) with all three electrode return configurations found to exhibit various degrees of retinal selectivity. CG and HX configurations were found to have a significantly higher degree of retinal selectivity compared to the MPV return ($p < 0.001$). The HX return configuration was found to also have significantly higher retinal selectivity than the CG return ($p < 0.05$). A significant difference in retinal selectivity was also observed between the MPV and MPR return configurations (figure 8(b); $p < 0.01$. n = 209 cortical sites).

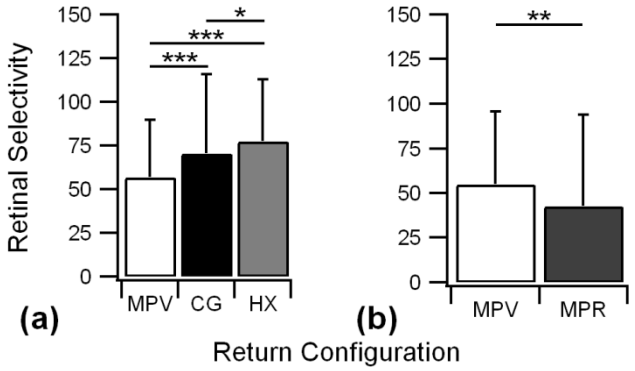

Figure 8: *Retinal selectivity (mean + SD) calculated by the percentage drop in spiking activity for each cortical recording location. Retinal selectivity was measured at the P90 current level of the BRE, elicited by stimulation of retinal electrodes located within 1mm from the BRE. (a) MPV versus CG versus HX electrode return configurations and (b) MPV versus MPR electrode return configurations. *p < 0.05. **p < 0.01. ***p < 0.001.*

Cortical Selectivity

An example of MUA captured with a 6x10 planar recording array following electrical stimulation of a single retinal electrode in three return configurations is shown in figure 9. This example reflects a retinal electrode which showed a high degree of cortical selectivity. The pattern of spiking activity was found to be similar between the MPV, CG and HX return configurations.

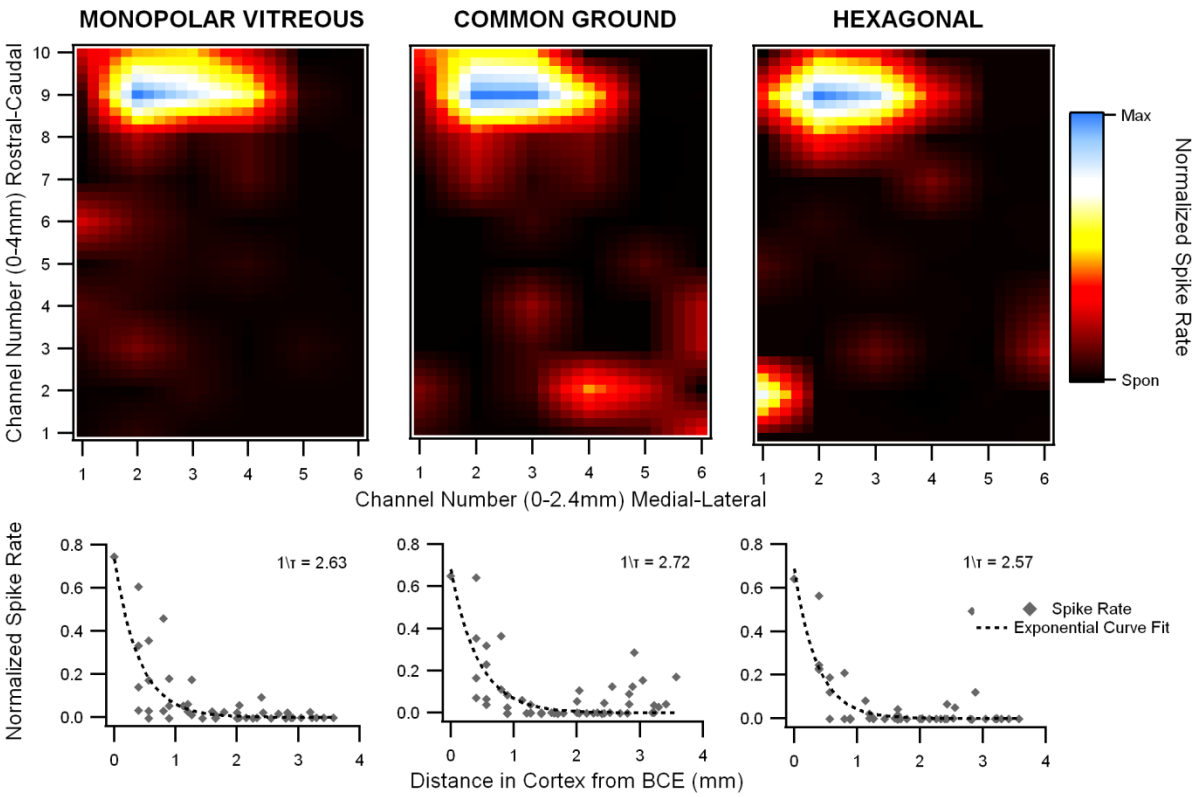

Figure 9: *Cortical spread of activation. The top panels demonstrate an example of normalized spiking activity patterns in the visual cortex for stimulation of one retinal electrode using the MPV, CG and HX return configurations at the P90 current level of the best cortical electrode (BCE). Beneath each image is a graph of normalized spike rate as a function of the distance in the cortex from the BCE (diamond symbols), fitted decaying exponential (dashed line) and corresponding inverse decay coefficient used to estimate cortical selectivity.*

At a near saturating stimulus level (equivalent to P90 of the BCE), no significant difference in the degree of cortical selectivity was found between the MPV, CG and HX return configurations (figure 10(a); n=14 retinal electrodes). Furthermore, no difference in cortical selectivity was observed between the MPV and MPR electrode configurations (figure 10(b); n=21) or between MPV and BP_*N* stimulation (figure 10(c); n=6). Although recordings were made from both cortical areas 17 and 18, we did not take into consideration the separate retinotopic maps of each area when computing cortical

selectivity. While we do not expect this to affect our pairwise analysis, the cortical selectivity of retinal electrodes which map to the area 17/18 transition zone may be reduced.

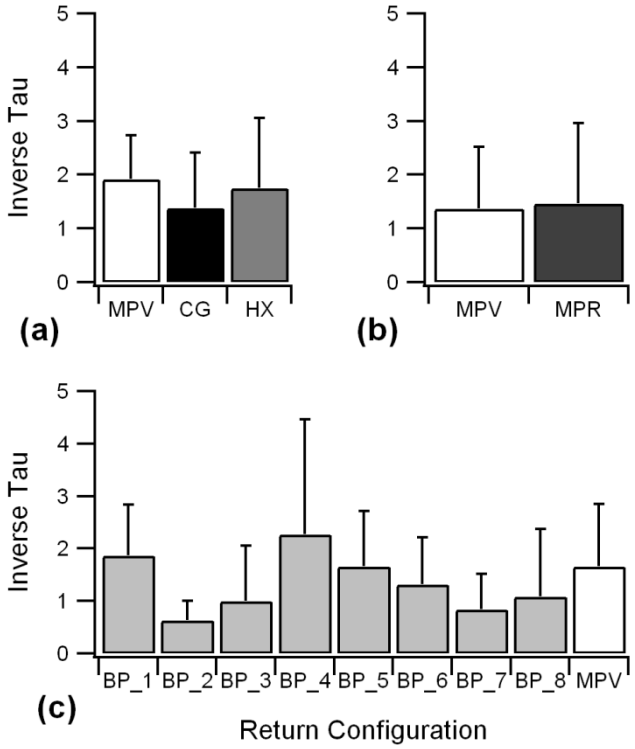

Figure 10: *Cortical selectivity (mean + SD). (a) MPV vs. CG vs. HX electrode return configurations, (b) MPV vs. MPR electrode return configurations and (c) BP_N vs. MPV electrode return configurations.*

Discussion

The aim of this study was to evaluate the efficacy of a variety of electrode return configurations for a suprachoroidal retinal array in inducing spatially selective MUA in V1 of the cat within safe levels of stimulating charge. We found that stimulation with a MPV return required lower charge and elicited cortical activity with a higher yield than either the CG or HX return configurations. We also found that retinal selectivity varied amongst the electrode return configurations whilst cortical selectivity did not. Furthermore, we found that MPR and BP_*N* stimulation with an active-return spacing greater than 2mm were generally as effective as that of a MPV return with the exception of the MPV return exhibiting higher retinal selectivity compared to the MPR return. We discuss the implications of these results on the design of a suprachoroidal retinal prosthesis and the benefits that they may provide to an eventual recipient of the implant.

Multi-Unit Cortical Activity

The presence of the two phases of MUA in our recordings is consistent with results from other retinal stimulation studies in cats: 6-20ms early component, 40-63ms late component (Elfar et al. 2009). It should be noted that the second phase of spiking was not always present in our cortical recordings and its presence was not dependent on the electrode return configuration. Recent *in vitro* retinal preparations in the healthy retina (Freeman and Fried 2011) have shown that retinal ganglion cells themselves show three phases of spiking activity separated in time in response to electrical stimulation. These phases have been classified as: 1) immediate spiking occurring within 6ms from stimulus onset and is attributed to direct activation of retinal ganglion cells, 2) early spiking (6-15ms from stimulus onset) thought to arise in response to indirect activation of retinal ganglion cells through activation of bipolar cells, and 3) late spiking occurring 40-55ms post-stimulus onset. It is possible that the first phase of spiking in V1 seen in this study (see figure 3(b)) is a result of both the immediate and early phases of spiking seen by Freeman and Fried (2011). This is yet to be demonstrated in an *in vivo* preparation and a study using various neurotransmitter blockers is required

to confirm the origin of the phases of spiking in V1. The second phase of spikes seen in V1 may have arisen from the late phase of Freeman and Fried (2011), however we cannot disregard that this phase of spiking may have arisen from cortical feedback (Elfar et al. 2009). From a perceptual viewpoint, patients do not report seeing two phosphenes in response to the electrical stimulation of a single retinal electrode. Therefore, it is unknown how the two phases of spiking evident in our cortical recordings would relate to perception. In the present paper, analysis was restricted to the early component.

P50 Charge Level

Studies with CIs have demonstrated that thresholds for both animal cortical recordings (Bierer and Middlebrooks 2002, Snyder et al. 2008, Fallon et al. 2009) and human psychophysics (Busby et al. 1994, Pfingst et al. 1995, Pfingst et al. 1997, Bierer 2007) decrease with increasing spread of electric field potential in the cochlea. Although we did not explicitly define the P50 charge level as threshold, a similar effect was seen with the HX and CG return configurations yielding higher P50 charge levels than the MPV return configuration, presumably due to a more restricted field spread in the retina,. Alternatively, the HX and CG return configurations could have resulted in more current shunting by the highly conductive choroidal blood vessels, thus not allowing current to effectively penetrate through the retina. The effects of current shunting have also been seen in simulations of subretinal stimulation (Ksai 2011) and *in vitro* subretinal stimulation (Gerdhart 2011).

Recently, it was reported that for suprachoroidal stimulation in cats, thresholds for evoked potentials were approximately three times higher with a HX return configuration than with a MPV return (Wong et al. 2009). Similarly, for *in vitro* subretinal electrical stimulation, approximately 6 times more charge was needed to stimulate the retina with a concentric ring return configuration (analogous to the HX return) compared to a monopolar return configuration (Gerhardt et al. 2011). In our study, we found that P50 charge level with the HX return configuration was almost double that of the MPV return configuration. The differences seen in relative charge levels between narrow and wide

electrode return configurations amongst the various studies is likely due in part to electrode spacing. As can be seen with the *BP_N* return configuration in our study (figure 4(c)), P50 charge levels were largest when the stimulating and return electrode were closely spaced possibly resulting in greater current shunting between the electrodes. In the studies by Gerhardt et al. (2011) and Wong et al. (2009) stimulating-return electrode separations used were 180µm and 600µm respectively while in this study electrodes were spaced 1000µm apart. These findings suggest that if a narrow configuration such as the HX or bipolar return is to be used in a retinal implant, careful consideration needs to be made with respect to electrode spacing on the retinal array.

Our results showed that the MPV return configuration had the lowest P50 charge level for neural activity. The corresponding mean charge density was 64±36µC cm^{-2} per phase. Despite differences in recording and analysis methods, this value is comparable to the thresholds reported in other retinal stimulation studies for measurements of evoked potentials with monopolar suprachoroidal stimulation of the retina: 42µC cm^{-2} (500µs pulse width, 100µm electrode diameter; (Sakaguchi et al. 2004)), 48.64 µC cm^{-2} (1ms pulse width, 750x300µm electrode site; (Zhou et al. 2008)) and 63.22 µC cm^{-2} (400µs pulse width, 230µm electrode diameter; (Wong et al. 2009)). The mean charge density in this study was also lower than our previously reported threshold charge density (115.06 µC $cm^{-}2$, 395 µm electrode diameter (Shivdasani et al. 2010)). This difference is likely due to evoked potential recordings and the use of coarse current steps (100-200µA), compared to the use of MUA recordings and finer current steps used in this study. As expected, due to the greater distance between the suprachoroidal array and the target retinal neurons (Kanda et al. 2004), our charge densities at the P50 charge level of the BCE were several times higher than those found previously *in vivo* with epiretinal (1-12 µC cm^{-2} per phase) (Walter and Heimann 2000) and subretinal (23 µC cm^{-2} per phase) (Yamauchi et al. 2005) stimulation.

Dynamic Range and Discriminability Index

Clinical studies have indicated that both the size and brightness of a phosphene is correlated with stimulating charge levels (Evans et al. 1979, De Balthasar et al. 2008, Wilke et al. 2011), although recently it has been reported that brightness can also be modulated by rate of stimulation (Nanduri et al. 2011). A larger dynamic range should therefore allow for more control over the phosphenes as it allows for more control of varying the injected charge. With CIs, it has been demonstrated that for sites in the auditory cortex most sensitive to electrical stimulation (equivalent to our BCEs), dynamic ranges are similar regardless of the electrode return configuration (Bierer and Middlebrooks 2002). We also observed comparable levels of dynamic range at the most sensitive site in the visual cortex among each of the electrode return configurations. This suggests that the range of operating currents over which brightness levels can be modulated may not be influenced by the choice of return. Little data exists on the dynamic range of electrical stimulation of the retina. However, the study by Stett et al. (2007) reported dynamic ranges (in absolute charge) of 1 to 10 nC for *in vitro*, subretinal electrical stimulation of the chicken retina. These values are much lower than the mean P10-P90 range of 79 nC obtained with the MPV return in this study, though, we report dynamic range of cortical neurons which may be different to those of retinal ganglion cells.

One must bear in mind the limitations of the definition for dynamic range used in this study. For the same P10-P90 charge range, recordings with a lower P50 charge are expected to have a larger dynamic range in dB units. Conversely, for the same value of dynamic range in dB, the recording with a higher P50 charge is expected to have a wider P10-P90 charge range. This is indeed the case with mean P10-P90 range observed to be smaller for the MPV return configuration (79 nC) compared to both the CG (125 nC) and the HX (114 nC) return configurations. This apparent bias between threshold and dynamic range has also been seen with subretinal electrical stimulation (Stett et al. 2007).

Although a wide dynamic range is beneficial to the modulation of brightness levels in a retinal implant, important also is the ability to produce a distinguishable level of brightness with a step increase in stimulating current. This was assessed by the discriminability index, d`, whereby discrimination between two current levels was performed on the basis of the MUA produced by each

current. The discrimination index for the MPV electrode configuration was approximately two fold greater compared to the narrower electrode configurations of BP_1, CG and HX. This result suggests that the step increase in current required to produce a change in brightness of a phosphene may be twice as large for the BP_1, CG and HX configurations compared to a MPV return. From our data we calculated that the minimum current step required to elicit distinguishable cortical responses (i.e. d`=1) was 41 µA, 75 µA and 73 µA for the MPV, CG and HX return configurations respectively. If we then take into consideration the P10-P90 operational range in which an electrode can be driven, then the potential number of brightness levels achievable was 4, 3, and 3 with the MPV, CG and HX return configurations respectively. Thus, even though MPV stimulation had a higher d`, it appears that the number of distinguishable brightness levels achievable with stimulation of a suprachoroidal retinal electrode is independent of electrode return configuration

Retinal and Cortical Selectivity

Retinal selectivity was measured by analyzing the drop in spike rate in V1 between all retinal electrodes adjacent to the BRE. Electrode return configuration was found to influence retinal selectivity, increasing from the MPV to the CG to the HX return. Based on the average retinal spread of activation we found that cortical sites were unable to respond to stimulation from retinal locations that were 1.5mm (MPV), 1mm (CG) and 0.99mm (HX) away from the BRE. Assuming a circular profile, we therefore estimated that the average "electrical receptive field" width for each cortical recording site in our study to be 12° of visual space for MPV stimulation and 7.9-8° for CG and HX stimulation (assuming 4° of visual space per millimeter, (Hubel and Wiesel 1959)). These widths are several times larger than the average receptive field width of cat cortical neurons measured with visual stimulation using a similar planar electrode array (1.6°, Warren et al. (2001)) and are also larger than visual receptive fields of some complex cells which can range up to 5° at an eccentricity between 10-15° (Wilson and Sherman 1976). The reason behind the differences between electrical and visual receptive fields of cortical neurons could be attributed to current spread in the retina. Our results

imply that the spread of current in the retina decreased from the MPV to the CG to the HX return. These results are in accordance with modeling studies (Lovell et al. 2006, Gerhardt et al. 2010, Wilke et al. 2011) that demonstrated a more confined electric field potential in the retina with narrow electrode configurations compared to monopolar stimulation. The degree of retinal current spread would be particularly important when employing simultaneous stimulation of multiple retinal electrodes. However, as the electric field produced from simultaneous stimulation of electrodes can be very unpredictable, this technique is rarely used in CIs (Seligman and Shepherd 2004). In this study, the increased current spread in the retina seen with MPV stimulation may cause summation of electric fields in the tissue distant to the stimulating electrodes (Gerhardt et al. 2010). This has been shown to cause limitations in spatial resolution and contrast sensitivity (Wilke et al. 2011) and as a result, phosphenes may appear fused. Based on these results one would presume that HX and CG stimulation would be more focused in the retina compared to MPV stimulation and may result in better spatial resolution. If MPV stimulation is to be employed in a retinal implant to take advantage of lower thresholds, retinal electrodes need to be separated by a further 2° (center-to-center spacing) compared to the HX return configuration to minimize the effects of current spread.

In contrast to retinal selectivity, we found that cortical selectivity was not dependent on electrode return configuration. Based on these results, one would expect each electrode return configuration to yield equally sized phosphenes in clinical use. These results were unexpected as given the higher retinal selectivity found with HX stimulation; one would predict a higher cortical selectivity. A previous study involving suprachoroidal stimulation in cats (Wong et al. 2009) reported that at matched current levels, HX stimulation activated a smaller area of V1 than MPV stimulation. At matching current levels, we would also expect to see lower cortical selectivity with the MPV return than with either CG or HX return configurations. However, we measured cortical selectivity at the same point along the dynamic range for each of the three return modes which took into consideration differences in the P50 charge level of each electrode return configuration and hence yielded contrasting results to those found in Wong et al (2009).

Our results at first would also seem to be in contrast to what has generally been observed in animals implanted with CIs, where narrow electrode configurations yield more spatially selective auditory cortical responses. For example, Bierer and Middlebrooks (2002) reported that the profile of MUA over time was most compact with a tripolar return configuration (analogous to the HX return configuration) and widest with the monopolar return. However, more recently, it was reported that at suprathreshold charge levels, no difference was found in the area of the auditory cortex activated following monopolar and CG stimulation (Fallon et al. 2009). In addition, discrimination by primates of auditory cues, presented at equivalent levels within the dynamic range was found to be affected only slightly or not at all by electrode return configuration (Morris and Pfingst 2000). Finally, despite improved spatial selectivity with narrow electrode configurations in animal models, such configurations have not resulted in greater speech recognition with CIs (Zwolan et al. 1996, Pfingst et al. 1997, Mens and Berenstein 2005, Berenstein et al. 2008). These drawings from the CI literature further support the hypothesis that electrode return configuration will have little effect on the spatial distribution of the percept induced in a retinal implant recipient.

Previous attempts to estimate that area of cortical activation from evoked potential recordings following electrical stimulation of the retina have reported that in cats, epiretinal (100μm platinum disk electrodes) and subretinal stimulation (100x100μm rectangular electrodes) activate approximately 2.7 mm and 1.7 mm width of cortex respectively (Eckhorn et al. 2006). These equate to approximately 3.8° and 2.4° of a visual angle respectively. In our study based on the inverse decay constant obtained with the MPV return ($1/\tau = 1.9$), suprachoroidal stimulation of one retinal site yielded MUA in 3.2 mm of cat cortex. If we define the limits of cortical activation to be the distance at which spontaneous spiking activity is reached (i.e. 3τ), and after normalizing for the eccentricity of the average location of the retinal electrodes included for analysis, this would equate to 4.5° of a visual angle (cortical magnification factor of 0.707 mm of cortex/degree of visual field (Tusa et al. 1978) for an eccentricity of 10°). This estimate implies that our cortical spread of activation results were of a similar order of magnitude to that achieved with both epiretinal and subretinal stimulation.

However given the differences in the recording type and methods used to estimate the width of cortical activation it is difficult to compare between studies.

Location of Monopolar Return Electrode

Retinal stimulation in rabbits (Shah et al. 2006) and cats (Shivdasani et al. 2010) have shown that the site of the monopolar return had no effect on the thresholds of electrically evoked potentials in the visual cortex.. In agreement with what has previously been seen in rabbits and cats, comparisons of P50 charge levels for MPR stimulation were not found to be different compared to MPV stimulation. Cortical selectivity was also comparable between the two locations of monopolar returns. Despite similarities in activation charge and cortical selectivity there was a reduction in retinal selectivity for the MPR return, likely due to better current penetration and/or less current spread through the retinal layers achieved with the MPV return placed in the vitreous humor. Furthermore, with CIs where stimulation with *BP_N* electrode configurations has been extensively studied, it has been shown that thresholds are comparable to those achieved with monopolar stimulation as the distance between the active and return electrodes is increased (Pfingst et al. 1995). In this study, we observed that with the BP_*N* configuration using active-return electrode separations of at least 3mm, P50 charge levels, dynamic ranges and cortical selectivity were found to be equivalent to those achieved with MPV stimulation. These results provide an avenue for an alternative location for a monopolar return either extraocularly or on the suprachoroidal array itself at a minimum distance of 3mm from any other electrode.

Further considerations in a blind model

This study was performed in a normally sighted animal model and further considerations need to be given as to how these results will relate to a blind animal model and subsequently a blind RP patient. For example, based on CI studies in normal hearing and deafened animals (Fallon et al, 2009); we

expect P50 charge levels to increase in the blind model as the number of target neurons decrease. This has been confirmed for monopolar stimulation of the retina in normal and Royal College of Surgeon rats (Kanda et al. 2004), where thresholds in the blind model were found to be almost twice those in the normally sighted model. More recently, it has been shown that thresholds continue to increase with prolonged periods of retinal degeneration in S334ter line 3 (RD) rats (Chan et al. 2008, Chan et al. 2011) and have been correlated with the extent of retinal ganglion cell loss (Chan et al. 2011). Also, the choroidal thickness in the cat is approximately 50µm (unpublished data) compared to approximately 200µm at the fovea of an RP patient (Ayton et al. 2011). Therefore it is anticipated that more current will be required to pass through the thicker choroid layer in humans in order to electrically stimulate retinal ganglion cells, possibly resulting in higher thresholds in humans than the P50 charge levels observed in this study. Furthermore, the experiments in the present study were only conducted over a duration of 3-4 days and we did not account for any long-term inflammatory changes that may take place in the suprachoroidal space or the retina with chronic implantation of an electrode array such as formation of an additional fibrous tissue layer and gliosis (Grill and Mortimer 1994, Duan et al. 2004). Given the relatively high thresholds and low yield of cortical responses resulting from CG and HX stimulation in our study, it remains to be seen whether we can achieve perceptual thresholds in chronically implanted blind humans within safe charge density limits using these electrode return configurations.

Cortical spread of activation and the resultant cortical selectivity is also likely to be influenced by changes occurring in an RP affected retina. For CI stimulation, compared to a normally hearing animal, the area of the cortex activated is approximately 3 times greater in a deafened animal (Fallon et al. 2009). Furthermore, preliminary investigations have shown that for suprachoroidal stimulation, activation of the superior colliculus is 2 times greater in the blind animal model compared to normally sighted animals (Kanda et al. 2004). It remains to be seen if electrode return configuration will influence spread of cortical activation in the blind animal model.

Summary

In this study, for a normally sighted animal model, electrode return configuration was found to have no bearing on dynamic range, the number of distinguishable brightness levels which may be encoded and cortical selectivity. Electrode return configuration was found to impact upon P50 charge levels and retinal selectivity. Our results indicate that choice of return configuration requires a trade-off between stimulating charge levels required to achieve phosphenes, and spatial resolution. The HX and CG configurations may provide superior spatial resolution compared to the MPV configuration, however, this needs to be balanced against safety issues, namely the ability to ensure that stimulation occurs within safe levels and does not exceed the voltage compliance limits of the stimulator.

Acknowledgements

We wish to thank Mark Harrison and David Ng for designing the flexible electrode arrays, Sam John, Tom Landry and Joel Villalobos for assistance with data collection, and Alexia Freemantle, Michelle McPhedran, David Nayagam and Merri Basa for technical assistance. We also wish to thank Prof. Dexter Irvine for reviewing earlier versions of this manuscript and the insights provided by the reviewers. This study was conducted at the Bionics Institute at St Vincent's Hospital and the Biological Research Centre at the Royal Victorian Eye and Ear Hospital. This research was supported by the Australian Research Council (ARC) through its Special Research Initiative (SRI) in Bionic Vision Science and Technology to Bionic Vision Australia and the Bertalli Family Foundation to the Bionics Institute. The Bionics Institute acknowledges the support it receives from the Victorian Government through its Operational Infrastructure Support Program. CERA receives Operational Infrastructure Support from the Victorian Government.

References

Ayton L N, Luu C D and Guymer R H (2011) Choroidal Thickness in Retinitis Pigmentosa. *ARVO 2011*

Berenstein C K, Mens L H, Mulder J J and Vanpoucke F J (2008) Current steering and current focusing in cochlear implants: comparison of monopolar, tripolar, and virtual channel electrode configurations. *Ear Hear* **29**:250-60

Bierer J A (2007) Threshold and channel interaction in cochlear implant users: evaluation of the tripolar electrode configuration. *J Acoust Soc Am* **121**:1642-53

Bierer J A and Middlebrooks J C (2002) Auditory cortical images of cochlear-implant stimuli: dependence on electrode configuration. *J Neurophysiol* **87**:478-92

Brummer S B and Turner M J (1977) Electrochemical Considerations for Safe Electrical Stimulation of the Nervous System with Platinum Electrodes. *Biomedical Engineering, IEEE Transactions on* **BME-24**:59-63

Busby P A, Whitford L A, Blamey P J, Richardson L M and Clark G M (1994) Pitch perception for different modes of stimulation using the cochlear multiple-electrode prosthesis. *J Acoust Soc Am* **95**:2658-69

Chan L H, Ray A, Thomas B B, Humayun M S and Weiland J D (2008) In vivo study of response threshold in retinal degenerate model at different degenerate stages. *Conf Proc IEEE Eng Med Biol Soc* **2008**:1781-4

Chan L L, Lee E J, Humayun M S and Weiland J D (2011) Both electrical stimulation thresholds and SMI-32-immunoreactive retinal ganglion cell density correlate with age in S334ter line 3 rat retina. *J Neurophysiol* **105**:2687-97

De Balthasar C, Patel S, Roy A, Freda R, Greenwald S, Horsager A, Mahadevappa M, Yanai D, Mcmahon M J, Humayun M S, Greenberg R J, Weiland J D and Fine I (2008) Factors affecting perceptual thresholds in epiretinal prostheses. *Invest Ophthalmol Vis Sci* **49**:2303-14

Dommel N, Suaning G J, Preston P, Lehmann T and Lovell N H (2005) In-Vitro Testing of Simultaneous Charge Injection and Recovery in a Retinal Neuroprosthesis *Engineering in Medicine and Biology Society, 2005 IEEE-EMBS 2005 27th Annual International Conference of the* 7612-5

Dommel N B and Et Al. (2009) A CMOS retinal neurostimulator capable of focussed, simultaneous stimulation. *Journal of Neural Engineering* **6**:035006

Duan Y Y, Clark G M and Cowan R S (2004) A study of intra-cochlear electrodes and tissue interface by electrochemical impedance methods in vivo. *Biomaterials* **25**:3813-28

Eckhorn R, Wilms M, Schanze T, Eger M, Hesse L, Eysel U T, Kisvarday Z F, Zrenner E, Gekeler F, Schwahn H, Shinoda K, Sachs H and Walter P (2006) Visual resolution with retinal implants estimated from recordings in cat visual cortex. *Vision Res* **46**:2675-90

Eckmiller R (1997) Learning retina implants with epiretinal contacts. *Ophthalmic Res* **29**:281-9

Elfar S D, Cottaris N P, Iezzi R and Abrams G W (2009) A cortical (V1) neurophysiological recording model for assessing the efficacy of retinal visual prostheses. *J Neurosci Methods* **180**:195-207

Evans J R, Gordon J, Abramov I, Mladejovsky M G and Dobelle W H (1979) Brightness of phosphenes elicited by electrical stimulation of human visual cortex. *Sens Processes* **3**:82-94

Fallon J B, Irvine D R and Shepherd R K (2009) Cochlear implant use following neonatal deafness influences the cochleotopic organization of the primary auditory cortex in cats. *J Comp Neurol* **512**:101-14

Freeman D K and Fried S I (2011) Multiple components of ganglion cell desensitization in response to prosthetic stimulation. *J Neural Eng* **8**:016008

Fujikado T, Kamei M, Sakaguchi H, Kanda H, Morimoto T, Ikuno Y, Nishida K, Kishima H, Maruo T, Konoma K and Ozawa M (2011) Testing of Semi-chronically Implanted Retinal Prosthesis by Suprachoroidal-Transretinal Stimulation in Patients with Retinitis Pigmentosa. *Invest Ophthalmol Vis Sci*

Gekeler F, Kopp A, Sachs H, Besch D, Greppmaier U, Zrenner E, Bartz-Schmidt K U and Szurman P (2010) Visualisation of active subretinal implants with external connections by high-resolution CT. *Br J Ophthalmol* **94**:843-7

Gerding H (2007) A new approach towards a minimal invasive retina implant. *J Neural Eng* **4**:S30-7

Gerhardt M, Alderman J and Stett A (2010) Electric field stimulation of bipolar cells in a degenerated retina--a theoretical study. *IEEE Trans Neural Syst Rehabil Eng* **18**:1-10

Gerhardt M, Groeger G and Maccarthy N (2011) Monopolar vs. bipolar subretinal stimulation-an in vitro study. *J Neurosci Methods* **199**:26-34

Grill W M and Mortimer J T (1994) Electrical properties of implant encapsulation tissue. *Ann Biomed Eng* **22**:23-33

Hartong D T, Berson E L and Dryja T P (2006) Retinitis pigmentosa. *Lancet* **368**:1795-809

Hubel D H and Wiesel T N (1959) Receptive fields of single neurones in the cat's striate cortex. *The Journal of Physiology* **148**:574-91

Humayun M S, De Juan E, Jr., Weiland J D, Dagnelie G, Katona S, Greenberg R and Suzuki S (1999) Pattern electrical stimulation of the human retina. *Vision Res* **39**:2569-76

Humayun M S, Dorn J D, Ahuja A K, Caspi A, Filley E, Dagnelie G, Salzmann J, Santos A, Duncan J, Dacruz L, Mohand-Said S, Eliott D, Mcmahon M J and Greenberg R J (2009) Preliminary 6 month results from the Argus II epiretinal prosthesis feasibility study. *Conf Proc IEEE Eng Med Biol Soc* **2009**:4566-8

Humayun M S, Weiland J D, Fujii G Y, Greenberg R, Williamson R, Little J, Mech B, Cimmarusti V, Van Boemel G, Dagnelie G and De Juan E (2003) Visual perception in a blind subject with a chronic microelectronic retinal prosthesis. *Vision Res* **43**:2573-81

John S E, Shivdasani M N, Leuenberger J, Fallon J B, Shepherd R K, Millard R E, Rathbone G D and Williams C E (2011) An automated system for rapid evaluation of high-density electrode arrays in neural prostheses. *J Neural Eng* **8**:036011

Jolly C N, Spelman F A and Clopton B M (1996) Quadrupolar stimulation for Cochlear prostheses: modeling and experimental data. *IEEE Trans Biomed Eng* **43**:857-65

Kanda H, Morimoto T, Fujikado T, Tano Y, Fukuda Y and Sawai H (2004) Electrophysiological studies of the feasibility of suprachoroidal-transretinal stimulation for artificial vision in normal and RCS rats. *Invest Ophthalmol Vis Sci* **45**:560-6

Kelly S K, Shire D B, Chen J, Doyle P, Gingerich M D, Drohan W A, Theogarajan L S, Cogan S F, Wyatt J L and Rizzo J F, 3rd (2009) Realization of a 15-channel, hermetically-encased wireless subretinal prosthesis for the blind. *Conf Proc IEEE Eng Med Biol Soc* **2009**:200-3

Klauke S, Goertz M, Rein S, Hoehl D, Thomas U, Eckhorn R, Bremmer F and Wachtler T (2011) Stimulation with a wireless intraocular epiretinal implant elicits visual percepts in blind humans. *Invest Ophthalmol Vis Sci* **52**:449-55

Kral A, Hartmann R, Mortazavi D and Klinke R (1998) Spatial resolution of cochlear implants: the electrical field and excitation of auditory afferents. *Hear Res* **121**:11-28

Lovell N H, Hallum L E, Chen S C, Dokos S, Byrnes-Preston P, Green R, Poole-Warren L, Lehmann T and Suaning G J (2006) *Advances in Retinal Neuroprosthetics* In: *Handbook of Neural Engineering* Place John Wiley & Sons, Inc. 337-56

Macmillan N A and Creelman C D (2005) *Detection theory : a user's guide* Editor Place Mahwah, N.J. Lawrence Erlbaum Associates

Mens L H and Berenstein C K (2005) Speech perception with mono- and quadrupolar electrode configurations: a crossover study. *Otol Neurotol* **26**:957-64

Middlebrooks J and Snyder R (2007) Auditory Prosthesis with a Penetrating Nerve Array. *JARO - Journal of the Association for Research in Otolaryngology* **8**:258-79

Mokwa W, Goertz M, Koch C, Krisch I, Trieu H K and Walter P (2008) Intraocular epiretinal prosthesis to restore vision in blind humans. *Conf Proc IEEE Eng Med Biol Soc* **2008**:5790-3

Morris D J and Pfingst B E (2000) Effects of electrode configuration and stimulus level on rate and level discrimination with cochlear implants. *J Assoc Res Otolaryngol* **1**:211-23

Nanduri D, Fine I, Horsager A, Boynton G M, Humayun M S, Greenberg R J and Weiland J D (2011) Frequency and amplitude modulation have different effects on the percepts elicited by retinal stimulation. *Invest Ophthalmol Vis Sci*

Pfingst B E, Miller A L, Morris D J, Zwolan T A, Spelman F A and Clopton B M (1995) Effects of electrical current configuration on stimulus detection. *Ann Otol Rhinol Laryngol Suppl* **166**:127-31

Pfingst B E, Zwolan T A and Holloway L A (1997) Effects of stimulus configuration on psychophysical operating levels and on speech recognition with cochlear implants. *Hearing Research* **112**:247-60

Rizzo J F, 3rd, Wyatt J, Loewenstein J, Kelly S and Shire D (2003) Methods and perceptual thresholds for short-term electrical stimulation of human retina with microelectrode arrays. *Invest Ophthalmol Vis Sci* **44**:5355-61

Rizzo J F, 3rd, Wyatt J, Loewenstein J, Kelly S and Shire D (2003) Perceptual efficacy of electrical stimulation of human retina with a microelectrode array during short-term surgical trials. *Invest Ophthalmol Vis Sci* **44**:5362-9

Sakaguchi H, Fujikado T, Fang X, Kanda H, Osanai M, Nakauchi K, Ikuno Y, Kamei M, Yagi T, Nishimura S, Ohji M and Tano Y (2004) Transretinal electrical stimulation with a suprachoroidal multichannel electrode in rabbit eyes. *Jpn J Ophthalmol* **48**:256-61

Seligman P M and Shepherd R K (2004) *Cochlear Implants* In: *Neuroprosthetics: Theory and Practice* Kenneth W. Horch, G S D Place World Scientific Pub Co Inc 2

Shah H A, Montezuma S R and Rizzo J F, 3rd (2006) In vivo electrical stimulation of rabbit retina: effect of stimulus duration and electrical field orientation. *Exp Eye Res* **83**:247-54

Shivdasani M N, Luu C D, Cicione R, Fallon J B, Allen P J, Leuenberger J, Suaning G J, Lovell N H, Shepherd R K and Williams C E (2010) Evaluation of stimulus parameters and electrode geometry for an effective suprachoroidal retinal prosthesis. *J Neural Eng* **7**:036008

Snider R S and Niemer W T (1961) *A stereotaxic atlas of the cat brain* Editor Place [Chicago Univ. of Chicago Press

Snyder R L, Middlebrooks J C and Bonham B H (2008) Cochlear implant electrode configuration effects on activation threshold and tonotopic selectivity. *Hear Res* **235**:23-38

Stett A, Mai A and Herrmann T (2007) Retinal charge sensitivity and spatial discrimination obtainable by subretinal implants: key lessons learned from isolated chicken retina. *J Neural Eng* **4**:S7-16

Suaning G and Lovell N H (2006) Electrode multiplexing method for retinal prosthesis *Journal*

Tusa R J, Palmer L A and Rosenquist A C (1978) The retinotopic organization of area 17 (striate cortex) in the cat. *J Comp Neurol* **177**:213-35

Van Den Honert C and Stypulkowski P H (1987) Single fiber mapping of spatial excitation patterns in the electrically stimulated auditory nerve. *Hear Res* **29**:195-206

Villalobos J, Allen P J, Mccombe M F, Ulaganathan M, Zamir E, Ng D C, Shepherd R K and Williams C E (2011) Development of a surgical approach for a wide-view suprachoroidal retinal prosthesis: evaluation of implantation trauma. *Graefes Arch Clin Exp Ophthalmol*

Walter P and Heimann K (2000) Evoked cortical potentials after electrical stimulation of the inner retina in rabbits. *Graefes Arch Clin Exp Ophthalmol* **238**:315-8

Wilke R, Gabel V P, Sachs H, Bartz-Schmidt K U, Gekeler F, Besch D, Szurman P, Stett A, Wilhelm B, Peters T, Harscher A, Greppmaier U, Kibbel S, Benav H, Bruckmann A, Stingl K, Kusnyerik A and Stingl K (2011) Spatial Resolution and Perception of Patterns Mediated by a Subretinal 16-Electrode Array in Patients Blinded by Retinal Dystrophies. *Invest Ophthalmol Vis Sci (Accepted June 2011)*

Wilke R G, Moghadam G K, Lovell N H, Suaning G J and Dokos S (2011) Electric crosstalk impairs spatial resolution of multi-electrode arrays in retinal implants. *J Neural Eng* **8**:046016

Wilson J R and Sherman S M (1976) Receptive-field characteristics of neurons in cat striate cortex: Changes with visual field eccentricity. *J Neurophysiol* **39**:512-33

Wong Y T, Chen S C, Seo J M, Morley J W, Lovell N H and Suaning G J (2009) Focal activation of the feline retina via a suprachoroidal electrode array. *Vision Res* **49**:825-33

Yamauchi Y, Franco L M, Jackson D J, Naber J F, Ziv R O, Rizzo J F, Kaplan H J and Enzmann V (2005) Comparison of electrically evoked cortical potential thresholds generated with subretinal or suprachoroidal placement of a microelectrode array in the rabbit. *J Neural Eng* **2**:S48-56

Yanai D, Weiland J D, Mahadevappa M, Greenberg R J, Fine I and Humayun M S (2007) Visual performance using a retinal prosthesis in three subjects with retinitis pigmentosa. *Am J Ophthalmol* **143**:820-7

Zhou J A, Woo S J, Park S I, Kim E T, Seo J M, Chung H and Kim S J (2008) A suprachoroidal electrical retinal stimulator design for long-term animal experiments and in vivo assessment of its feasibility and biocompatibility in rabbits. *J Biomed Biotechnol* **2008**:547428

Zrenner E, Miliczek K D, Gabel V P, Graf H G, Guenther E, Haemmerle H, Hoefflinger B, Kohler K, Nisch W, Schubert M, Stett A and Weiss S (1997) The development of subretinal microphotodiodes for replacement of degenerated photoreceptors. *Ophthalmic Res* **29**:269-80

Zwolan T A, Kileny P R, Ashbaugh C and Telian S A (1996) Patient Performance with the Cochlear Corporation "20 + 2" Implant: Bipolar Versus Monopolar Activation. *Otology & Neurotology* **17**:717-23